Published OnlineFirst May 23, 2017; DOI: 10.1158/0008-5472.CAN-16-2165

Microenvironment and Immunology

Cancer Research

Immune Checkpoint Blockade, Immunogenic Chemotherapy or IFN-α Blockade Boost the Local and Abscopal Effects of Oncolytic Virotherapy

Laetitia Fend[1,2], Takahiro Yamazaki[2,3,4], Christelle Remy[1], Catherine Fahrner[1], Murielle Gantzer[1], Virginie Nourtier[1], Xavier Préville[1,5], Eric Quéméneur[1], Oliver Kepp[6,7,8,9,10], Julien Adam[2,11], Aurélien Marabelle[12], Jonathan M. Pitt[2,3,4], Guido Kroemer[6,7,8,9,10,13,14], and Laurence Zitvogel[2,3,4,11,15]

Abstract

Athough the clinical efficacy of oncolytic viruses has been demonstrated for local treatment, the ability to induce immune-mediated regression of distant metastases is still poorly documented. We report here that the engineered oncolytic vaccinia virus VV_{WR}-$TK^{-}RR^{-}$-Fcu1 can induce immunogenic cell death and generate a systemic immune response. Effects on tumor growth and survival was largely driven by $CD8^{+}$ T cells, and immune cell infiltrate in the tumor could be reprogrammed toward a higher ratio of effector T cells to regulatory $CD4^{+}$ T cells. The key role of type 1 IFN pathway in oncolytic virotherapy was also highlighted, as we observed a strong abscopal response in *Ifnar*$^{-/-}$ tumors. In this model, single administration of virus directly into the tumors on one flank led to regression in the contralateral flank. Moreover, these effects were further enhanced when oncolytic treatment was combined with immunogenic chemotherapy or with immune checkpoint blockade. Taken together, our results suggest how to safely improve the efficacy of local oncolytic virotherapy in patients whose tumors are characterized by dysregulated IFNα signaling. *Cancer Res; 77(15); 4146–57. ©2017 AACR.*

Introduction

Oncolytic virotherapy is an attractive and emerging modality for treating cancer, boosted by the recent approval of IMLYGIC (T-VEC/talimogene laherparepvec), a modified herpes simplex virus 1 encoding human GM-CSF, for use in stage III melanoma patients with injectable but nonresectable lesions in the skin and lymph nodes (1). The oncolytic viruses (OV) used in antitumoral therapies are nonpathogenic viral strains that selectively kill malignant cells upon replication, while sparing normal cells. This selective effect essentially results from the fact that tumor cells have a limited ability to respond to infection due to defects in their antiviral signaling pathways, such as the type I IFN signaling pathway (2, 3).

The original purpose during the early development of oncolytic virotherapy (in the 1990s) was to create OVs that could bypass tumor defense mechanisms with the aim of inducing massive cell death. It is now believed that this level of oncolytic activity can only occur in situations where both natural innate and adaptive antiviral responses are outpaced (2).

Many mechanisms indeed account for the tumoricidal activity of oncolytic viruses (4). Ras transformation promotes reovirus oncolysis by enhancing virion disassembly during entry, viral progeny production, virus release through apoptosis, and finally precludes IFN production following reovirus infection, permitting enhanced cell-to-cell virus spread (5–7). In addition, Roulstone and colleagues (8) reported that the combination of ERK1/2 inhibition and reovirus infection enhanced efficacy of reoviruses through ER stress–induced apoptosis. *In vivo*, combined treatments of RT3D and PLX4720 showed significantly increased activity in BRAF-mutant tumors in both immunodeficient and immunocompetent models, supporting clinical translation of strategies in which RT3D is combined with BRAF inhibitors (in BRAF-mutant melanoma) and/or MEK inhibitors (in BRAF- and RAS-mutant melanoma).

In the majority of cases, the most effective OV treatments combine potent viral oncolysis with induction of a specific immune response against tumor antigens, as shown in several clinical and preclinical studies (9–12). The mechanisms how OV therapies elicit antitumor immune responses are not clearly

[1]Transgene S.A., Illkirch-Graffenstaden, France. [2]Institut de Cancérologie Gustave Roussy Cancer Campus (GRCC), Villejuif, France. [3]INSERM Unit U1015, Villejuif, France. [4]Université Paris Sud, Université Paris-Saclay, Faculté de Médecine, Le Kremlin Bicêtre, France. [5]Amoneta Diagnostics, Huningue, France. [6]INSERM, U1138, Centre de Recherche des Cordeliers, Paris, France. [7]Equipe 11 Labellisée par la Ligue Nationale Contre le Cancer, Centre de Recherche des Cordeliers, Paris, France. [8]Université Paris Descartes/Paris V, Sorbonne Paris Cité, Paris, France. [9]Université Pierre et Marie Curie, Paris, France. [10]Metabolomics and Cell Biology Platforms, Villejuif, France. [11]Department of Pathology, GRCC, Villejuif, France. [12]DITEP (Département d'Innovations Thérapeutiques et Essais Précoces), Gustave Roussy, INSERM U1015, Villejuif, France [13]Pôle de Biologie, Hôpital Européen Georges Pompidou, AP-HP, Paris, France. [14]Karolinska Institute, Department of Women's and Children's Health, Karolinska University Hospital, Stockholm, Sweden. [15]Center of Clinical Investigations in Biotherapies of Cancer (CICBT) 1428, Villejuif, France.

Note: Supplementary data for this article are available at Cancer Research Online (http://cancerres.aacrjournals.org/).

Corresponding Author: Laurence Zitvogel, Gustave Roussy Cancer Campus, 114 rue Edouard Vaillant, 94805 Villejuif Cedex, France. Phone: 331-4211-5041; Fax: 331-4211-6094; E-mail: laurence.zitvogel@gustaveroussy.fr

doi: 10.1158/0008-5472.CAN-16-2165

Published OnlineFirst May 23, 2017; DOI: 10.1158/0008-5472.CAN-16-2165

understood yet, but likely involve the capture of released tumor antigens by bystander antigen-presenting cells (APC) following tumor cell lysis (13). The precise modality of elicited tumor cell death is then another important factor contributing to the efficacy of oncolytic virotherapy. The possibility that OVs induce immunogenic cell death (ICD), a cell death modality defined by the release of damage-associated molecular patterns (DAMP) from dying cells (14), has been previously suggested (2, 15). This form of cell death was originally observed to occur in tumor cells following administration of certain chemotherapeutic compounds, with striking similarities to the intracellular death circuitries activated during viral infections (14, 16). Hence, we wanted to substantiate this observation and confirm that ICD underlies the innate and adaptive antitumor responses in OV therapy. We also assessed the relation with IFN signaling pathway, another major determinant of the antiviral immune response (17).

Oncolytic viruses are usually administered intratumorally or peritumorally. Abscopal response is a rather rare phenomenon occurring in certain circumstances, such as in some metastatic melanoma patients treated with a combination of local irradiation and systemic anti-CTLA-4 immunomodulation (18–20). The ability to elicit abscopal effects, that is, regressions of tumors distant from the site of administration, implies the release of tumor-associated antigens at the site of oncolysis, in an environment therapeutically modulated to be immunogenic (2, 21, 22). Instances of systemic effects have been reported for OVs in the clinic (23–26), including T-VEC/talimogene laherparepvec, but the underlying immune mechanisms responsible for these effects remain a conundrum.

Another strategy to boost antitumor immune responses initiated by oncolytic virotherapy is to circumvent tolerance mechanisms (27). Thus, combination with immune checkpoint blockers (ICB) is a recent example that is currently under clinical investigation, with the intention to (re)activate otherwise dysfunctional TILs within tumor beds during oncolysis-derived inflammation and tumor antigen presentation by APCs (28).

TG6002 is an advanced OV currently being brought by Transgene S.A. into clinic. It would be important to demonstrate abscopal response in this perspective. TG6002 was designed on the vaccinia virus platform, in the Copenhagen strain, which is known to be more replicative in human, with two gene deletions conferring specific replication in tumor, that is, thymidine kinase and ribonucleotide reductase. As a complementary functional modality, it encodes FCUI, a chimeric enzyme converting the prodrug 5-FC into 5-FU (29). As the purpose was to assess the ability of OV to induce abscopal response in a syngenic preclinical model, we used a surrogate product competent for replication in mice, referred to as VV_{WR}/TK^-RR^-/FCU1 or WR, based on the Western Reserve strain (29). We here report on the ability of WR to induce several hallmarks of ICD in established tumors growing in mice. Moreover, we show that the antitumor immune response established by WR can be enhanced upon combination with either the ICD-inducing chemotherapy oxaliplatin, or the immune checkpoints blockers anti-CTLA-4 or anti-PD-1. Noteworthy, the combination with immune checkpoint blockade was associated with a significant improvement in regressions in distant untreated tumors. Finally, we show that these WR-mediated abscopal effects are greatly amplified when tumors are defective for the IFNAR signaling pathway.

Materials and Methods

Cell culture

Media and supplements for cell culture were obtained from Gibco-Life Technologies. All chemicals were obtained from Sigma-Aldrich and plastic ware was obtained from Corning BV Life Sciences. MCA205 fibrosarcoma cells ($H2^b$) were induced by 3-methylcholanthrene in C57BL/6 mice (30) and were regularly checked for histocompatibility. *Ifnar*$^{-/-}$ and *Tlr3*$^{-/-}$ MCA205 was generated with ZFN technology as described previously (31). Authenticated CT26 colorectal carcinoma ($H2^d$) and B16F10 ($H2^b$) melanoma cell lines were obtained from the ATCC in 1996. All cell lines were immediately amplified to constitute liquid nitrogen stocks and (upon thawing) never passaged for more than 1 month before use in experimental determinations, they were negative for known mouse pathogens, including mycoplasma. Tumor cells lines were cultured in RPMI1640 medium supplemented with 10% FCS, 2 mmol/L L-glutamine, 100 IU/mL penicillin G sodium salt, 100 μg/mL streptomycin sulfate, 1 mmol/L sodium pyruvate, and 1 mmol/L nonessential amino acids. Cells were grown at 37°C in a humidified incubator under a 5% CO_2 atmosphere.

Oncolytic vaccinia virus

WR (VV_{WR}/TK^-RR^-/FCU1) is an engineered vaccinia virus, Western Reserve strain, doubly deleted virus for thymidine kinase and ribonucleotide reductase, with *Fcu1* inserted at the *Tk* locus as described previously (15).

Mice

Mice were maintained in specific pathogen-free (SPF) conditions in a temperature-controlled environment with 12-hour light, 12-hour dark cycles, and received food and water *ad libitum*. Animal experiments followed the guidelines from Federation of European Laboratory Animal Science Association (FELASA), were compliant with EU Directive 63/2010, and were approved by the Ethical Committee of the Gustave Roussy Cancer Campus (Villejuif, France). Mice were used between 7 and 14 weeks of age. SPF C57BL/6 J and BALB/c mice were obtained from Envigo and Janvier, respectively, and were kept in SPF conditions at Gustave Roussy (Villejuif, France). *Tlr4*$^{-/-}$ BALB/c and *Ifnar*$^{-/-}$ C57BL/6 mice were bred and maintained in the animal facility of Gustave Roussy (Villejuif, France). *Ifnar*$^{-/-}$ C57BL/6 mice were kindly provided by the University of Montpellier (Montpellier, France).

Vaccination protocol

MCA205 cells were infected in suspension by WR at a multiplicity of infection (MOI) of 10^{-2}. After 20 hours, 10^6 cells (40% of dying cells) were injected into the right flank of C57BL/6 mice. After 10 days, mice were challenged with 5×10^5 untreated MCA205 cells into the left flank.

Tumor models

Mice were injected subcutaneously (s.c.) into the right flank with 8×10^5 WT, *Ifnar*$^{-/-}$, or *Tlr3*$^{-/-}$ MCA205 cells. Tumor cell lines were inoculated into WT-treated, or *Ifnar*$^{-/-}$ C57BL/6 mice. In a similar model, 8×10^5 CT26 cells were inoculated subcutaneously (right flank) into WT-treated or *Tlr4*$^{-/-}$ BALB/c mice. Tumor areas (longest dimension × perpendicular dimension) were routinely monitored by caliper. When tumors reached a size of 40 mm^2 (day 0), mice were administered intratumorally (i.t.)

Published OnlineFirst May 23, 2017; DOI: 10.1158/0008-5472.CAN-16-2165

2 times at 3-day intervals (day 0 and day 3) with 10^7 plaque-forming units (pfu) WR or with buffer, unless stated otherwise in the figure legends. In T-cell depletion experiments, anti-CD4 and anti-CD8 mAbs (GK1.5 and 53–6.72, respectively; 200 μg/mouse) or their isotype controls (LTF-2 and 2A3, respectively) were injected intraperitoneally (i.p.) 4 days before the first WR injection and continued at the same dose every 7 days. In IFNAR1-blocking experiments, mice were injected intraperitoneally with 2.5 mg/mouse of anti-IFNAR1 mAb (MAR1-5A3) at day 5 and 0.5 mg/mouse at day 10, or with isotype control mAb (mouse IgG1). To evaluate the therapeutic activity of WR in combination with chemotherapy, a single dose of oxaliplatin was injected intraperitoneally at day 0 (10 mg/kg/mouse) followed by 2 intratumoral treatments with 10^7 pfu/mouse of WR on day 5 and 8. To evaluate the therapeutic activity of WR in combination with immune checkpoint inhibitors, several experimental settings were evaluated. In the first setting, mice were injected intraperitoneally 3 times at 3-day intervals (day 0, 3, and 6) with 100 μg anti-CTLA4 mAb (9D9) or with 250 μg anti-PD-1 mAb (RMP1-14), or with relevant isotype control mAbs (MPC11 or 2A3) ahead of WR treatment at day 7 and 10. In the second setting, mice were first treated with WR (at day 0 and 3) and subsequently with the mAbs (at day 6, 9, and 12) at the aforementioned doses. In experiments examining abscopal effects of treatment, mice were subcutaneously injected into the right flank with 8×10^5 *Ifnar*$^{-/-}$ MCA205 cells, and injected into the left (contralateral) flank with 8×10^5 WT MCA205 cells to form a second tumor 3 days following inoculation of the first tumor. All mAbs for use *in vivo* were obtained from BioXcell, using the recommended isotype control mAbs.

Flow cytometry

Seven days after the first WR injection, tumors were harvested, cut into small pieces, and digested in RPMI1640 medium containing Liberase at 25 μg/mL (Roche) and DNase1 at 150 UI/mL (Roche) for 30 minutes at 37°C. The mixture was subsequently passaged through a 100-μm cell strainer. A total of 2×10^6 tumor cells were preincubated with purified anti-mouse CD16/CD32 (93; eBioscience) for 15 minutes at 4°C, before membrane staining. For intracellular staining, the FoxP3 staining kit (eBioscience) was used. Dead cells were excluded using the Live/Dead Fixable Yellow Dead Cell Stain Kit (Life Technologies). Anti-FoxP3 (FJK-16 s), anti-CTLA4 (UC10-4B9), anti-PD-1 (J43), and isotype controls IgG2b (eBRG2b) or Armenian Hamster IgG (eBio299Arm) were purchased from eBioscience. Anti-CD45 (30-F11), anti-CD3 (145-2C11), anti-CD8 (53-6.7), anti-CD25 (PC61.5.3), anti-NK1.1 (PK136), anti-Ly-6C (AL-21), and anti-F4/80 (BM8) were obtained from BD Biosciences. Anti-CD4 (GK1.5), anti-CD11b (M1/70), anti-PD-L1 (10F.9G2), and isotype control IgG2b (RTK4530) were purchased from Biolegend. A FACSCanto II flow cytometer (BD Biosciences) was used for eight-color flow cytometry acquisition. Analyses were performed using FACS Diva software.

HMGB1 quantification

CT26 and MCA205 cells were infected by WR in suspension at an MOI ranging from 10^{-1} to 10^{-4}, or were treated with 5 μmol/L doxorubicin (or PBS volume control). Cell supernatants were collected 48 hours after infection and HMGB1 was quantified by ELISA following the manufacturer's instructions (IBL International).

IFN type 1 quantification

Mice were injected subcutaneously into the right flank with 8×10^5 MCA205 cells. Tumor areas (longest dimension × perpendicular dimension) were routinely monitored by caliper. When tumors reached a size of 40 mm^2 (day 0), mice were administered intratumorally 2 times at 3-day intervals (day 0 and day 3) with 10^7 pfu WR or with buffer. Sera were harvested on day 1, 3, 5, 7, and 11 and IFNα and IFNβ serum levels were quantified by ProcartaPlex Multiplex Immunoassay following manufacturer's instructions (Thermo Fisher Scientific). Each bar represents the mean of 5 mice per group.

Statistical analysis

Where indicated, statistical analyses were performed using Prism 5 software (GraphPad). Data are represented as means ± SEM. Unpaired events were compared by Mann–Whitney test. Multiple comparisons were tested by Kruskal–Wallis test, followed by Dunn test to compare the different pairs. Comparisons of Kaplan–Meier survival curves were performed using the log-rank Mantel–Cox test. All reported tests are two-tailed and were considered significant at P values <0.05.

Results

As a control, we first assessed response in a prophylactic setting. C57BL/6 mice were vaccinated with WR-treated MCA205 cells in the left (ipsilateral) flank and challenged in the opposite (contralateral) flank 10 days later with untreated MCA205 cells (Fig. 1A). Inoculation with WR-treated MCA205 cells provided complete control of tumor growth on the ipsilateral flank, and displayed a significant control of contralateral tumors, as compared with the PBS-treated MCA205 cell control vaccine (Fig. 1A). In a therapeutic setting, WR was intratumorally injected into two models; (i) an established MCA205 sarcoma in C57BL/6 mice (Fig. 1B), or (ii) into an established CT26 carcinoma in BALB/c mice (Fig. 1C). In both cases, there was a benefit of WR, with significantly delayed tumor growth and enhanced survival, compared with controls.

This demonstration of abscopal response in contralateral tumors suggested the induction of an antitumor immune response. We therefore examined the involvement of CD4$^+$ and CD8$^+$ T cells in the therapeutic MCA205 model, through specific depletion using targeted mAbs (Fig. 2B). Depletion of CD8$^+$ T cells completely abolished the effect of WR, both in terms of tumor control and of survival. On the other hand, depletion of CD4$^+$ T cells had no effect. Taken together, these results hint that CD8$^+$ T-cell response is the major determinant to the systemic efficacy of WR.

Considering our previous findings in renal carcinoma cells, which linked the release of HMGB1, a prominent DAMP released during ICD (32), to increasing MOI of OV (15), we hypothesized that ICD induced by WR might be responsible for the generation of CD8$^+$ T cells. We here confirmed that HMGB1 was released from MCA205 upon treatment with WR, in a MOI-dependent fashion (Fig. 2C). TLR4 is the HMGB1-cognate receptor responsible for APC activation (14, 32). We also show that the therapeutic response elicited by WR was lost in BALB/c mice deficient for TLR4 (Fig. 2D). We could identify other hallmarks of DAMP after OV infection, that is, trends for increased calreticulin exposure (not shown), release of ATP and CXCL10 (33, 34) in the supernatants of WR-treated CT26

Published OnlineFirst May 23, 2017; DOI: 10.1158/0008-5472.CAN-16-2165

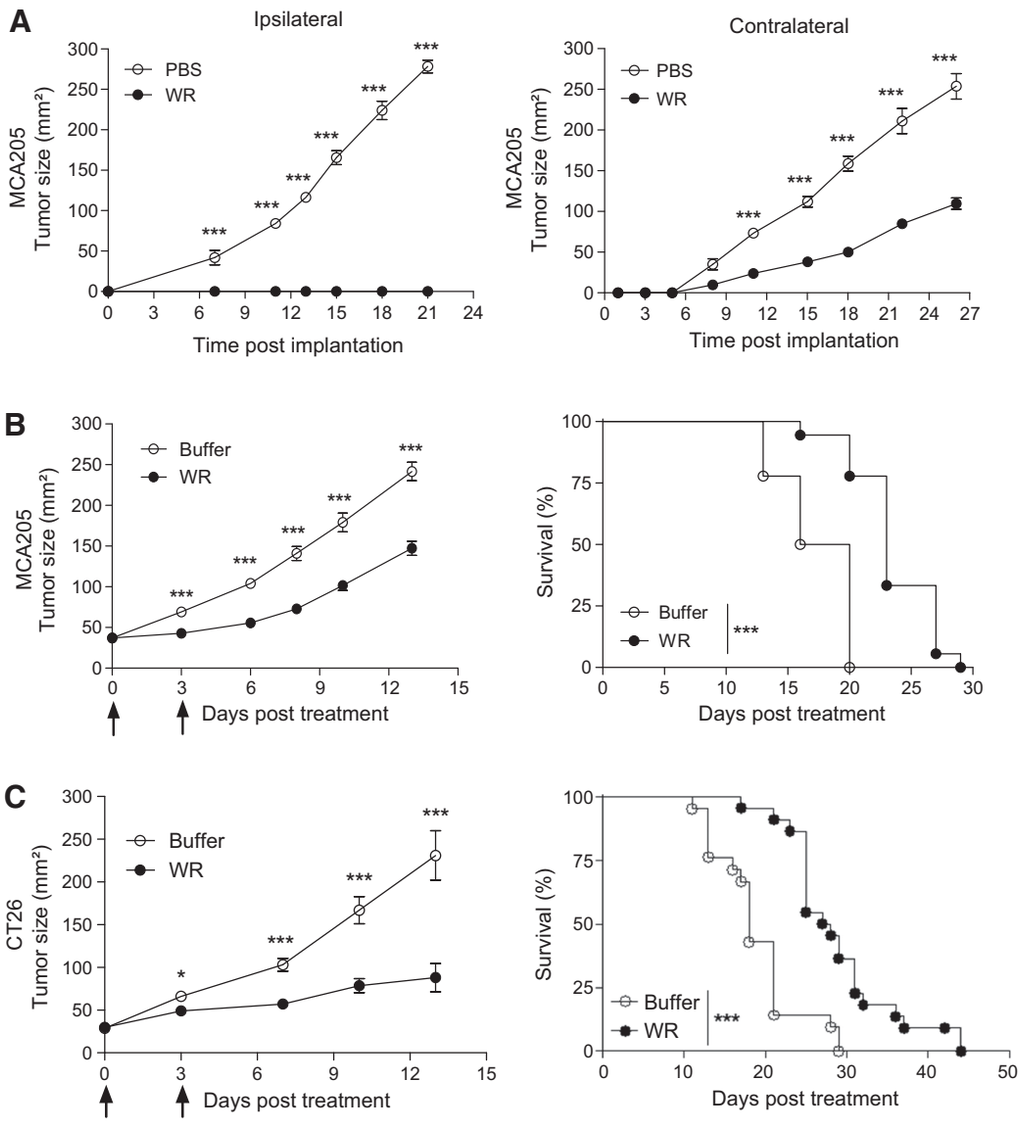

Figure 1.

WR-induced abscopal response in syngenic tumor models. **A,** C57BL/6 mice were vaccinated with 10^6 MCA205 tumor cells pretreated with either WR (solid symbol) or PBS as control (open symbol; left), then challenged 10 days later with untreated MCA205 (right). Tumor growth curves of the MCA205 vaccinations (ipsilateral) and the MCA205 challenge (contralateral) are depicted. **B,** C57BL/6 mice were implanted with 8×10^5 MCA205 tumor cells. When tumors reached approximately 40 mm^2, mice were intratumorally injected with 10^7 pfu WR, or with control buffer, on day 0 and day 3. **B,** Tumor size (left) and percentages of surviving mice (right) are depicted. **C,** BALB/c mice were implanted with 8×10^5 CT26 tumor cells and treated as in **B** with WR, or control buffer, on day 0 and day 3. Tumor size (left) and percentages of surviving mice (right) are shown. Data are representative of three independent experiments in **A** and **B**, and four representative experiments in **C**. Tumor size data depict the mean ± SEM. Each experiment contained 5–6 mice/group. ***, $P < 0.001$ by unpaired Mann–Whitney test, or by Kaplan–Meier analysis and log-rank Mantel–Cox test in **B** and **C** (right).

cells, and MCA205 cells, increased autophagy preceeding apoptosis (Supplementary Fig. S1).

Autocrine and paracrine type I IFN signaling among tumor cells has been established as another key factor contributing to the ICD induced by anthracyclines and oxaliplatin, in a pattern mimicking the one induced by viral pathogens (31). This prompted us to investigate the contribution of this signaling pathway in WR-mediated antitumor responses. The therapeutic efficacy of WR was assessed in two MCA205 clones generated to be deficient for type I IFN receptor (IFNAR) signaling ($Ifnar^{-/-}$). Both IFNAR2-deficient cell lines could be effectively treated *in vivo*, and in most cases completely regressed after intratumoral injection of WR (Fig. 3A). Of note, IFNAR-deficient tumors were much more sensitive to WR (Fig. 3A) than WT tumors (Fig. 1A).

Using qPCR as well as plaque assay on chicken embryo fibroblasts, we titrated viral replication *in vitro* postinfection of MCA205 WT versus $Ifnar^{-/-}$ cells with increasing colony-forming units of WRTG1737, but did not find that IFNAR deficiency facilitated

Published OnlineFirst May 23, 2017; DOI: 10.1158/0008-5472.CAN-16-2165

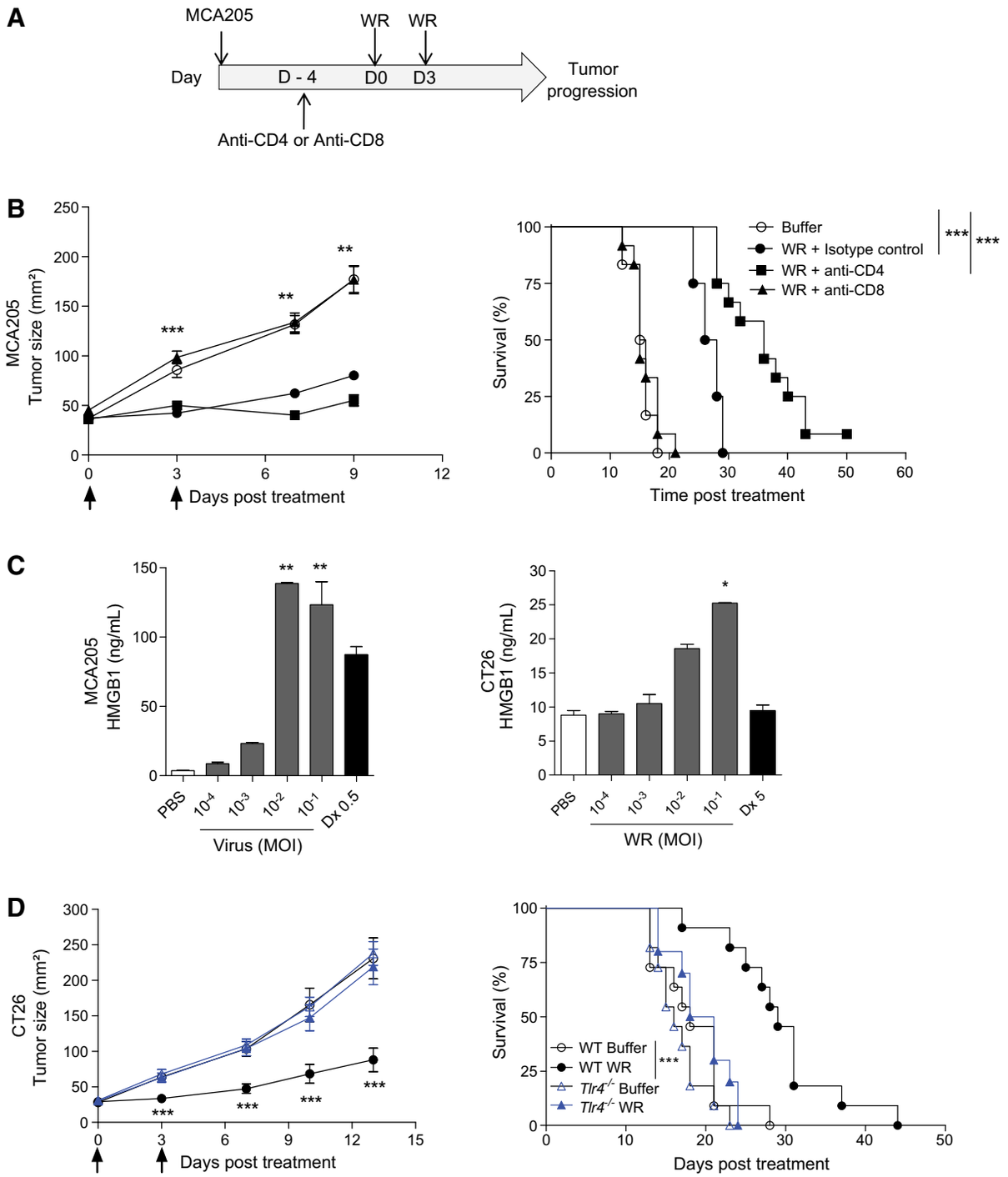

Figure 2.

The antitumor activity of WR is T-cell–dependent and is associated with immunogenic cell death. **A,** C57BL/6 mice were implanted with MCA205 cells and treated with anti-CD4 or anti-CD8 mAbs 4 days prior to start of treatment with WR. Mice were therapeutically treated with two intratumoral injections of 10^7 pfu WR or with control buffer on day 0 and day 3. Tumor size as mean ± SEM and percentages of surviving mice are depicted in **B**. **C,** Quantification by ELISA of HMGB1 in the supernatants of MCA205 cells and CT26 infected with WR or treated with PBS (control) or doxorubicin (0.5 μmol/L for MCA205 cells and 5 μmol/L for CT26 cells). **D,** WT or *Tlr4*$^{-/-}$ BALB/c mice were implanted with 8×10^5 CT26 tumor cells. When tumors reached approximately 40 mm^2, mice were intratumorally treated with 10^7 pfu WR or control buffer on day 0 and day 3. Tumor size and percentages of surviving mice are shown. Results represent at least two independent experiments of 5–6 mice/group in **B**–**D**. Tumor size and HMGB1 data depict the mean ± SEM. **, $P < 0.01$; ***, $P < 0.001$ by Kruskal–Wallis test followed by Dunn post test, or by Kaplan–Meier analysis and log-rank Mantel–Cox test in **B** and **D** (right). Dx, doxorubicin.

Published OnlineFirst May 23, 2017; DOI: 10.1158/0008-5472.CAN-16-2165

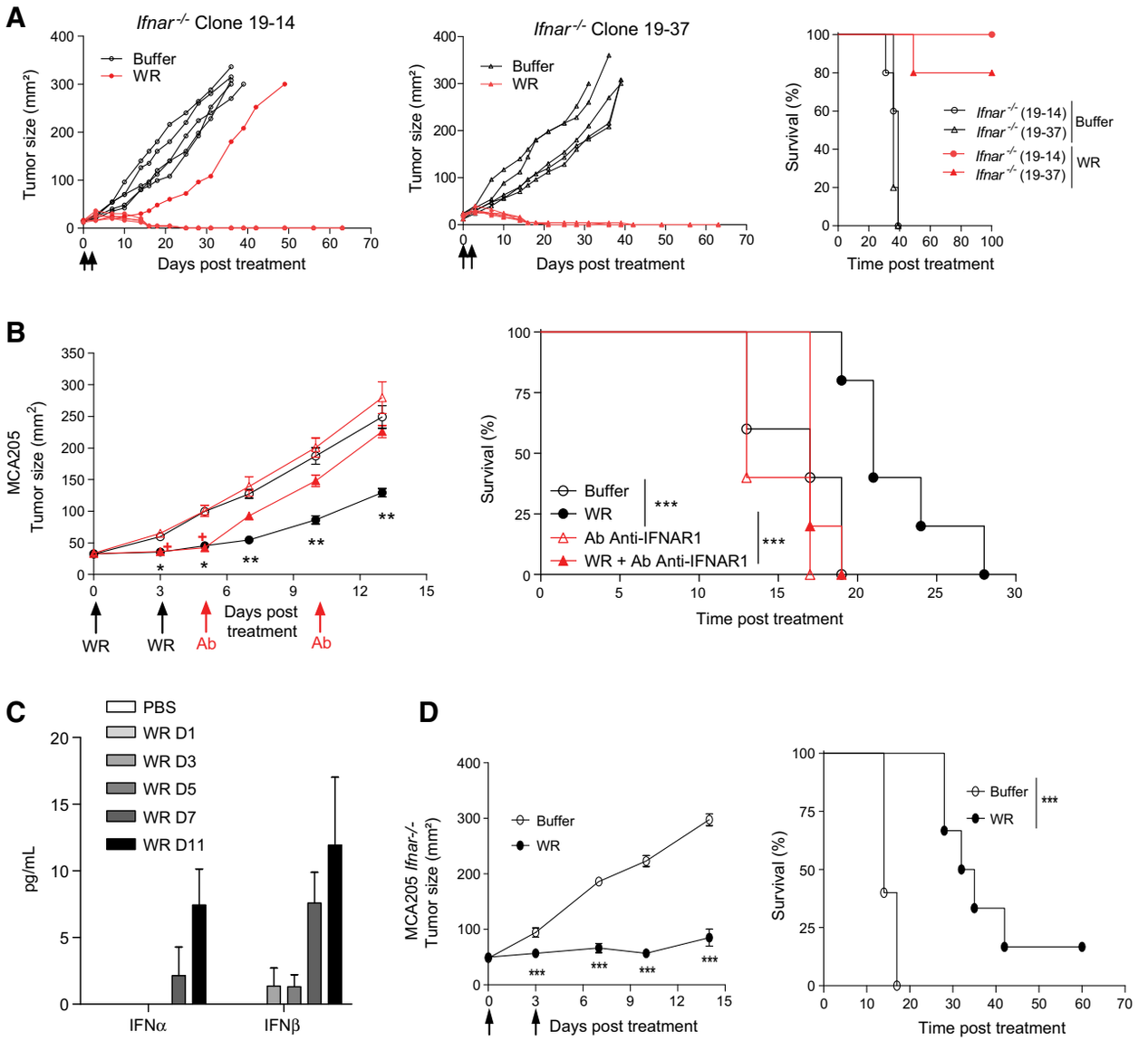

Figure 3.

The antitumor activity of WR is determined by IFNAR signaling. **A,** C57BL/6 mice were implanted with 8×10^5 of either *Ifnar*$^{-/-}$ MCA205 clone 19–14 (left) or *Ifnar*$^{-/-}$ MCA205 clone 19–37 (middle). When tumors reached approximately 40 mm^2, mice were intratumorally treated with 10^7 pfu WR or with control buffer on day 0 and day 3, and tumor growth was subsequently monitored. Percentages of surviving mice are depicted in the right panel of **A**. **B,** C57BL/6 mice bearing MCA205 tumors were treated with WR or buffer on day 0 and day 3, as described previously, and received anti-IFNAR1 mAb on days 5 and 10. Tumor size (left) and percentages of surviving mice (right) are shown. **C,** Serum concentrations of type 1 IFN during local WR infection. MCA205 WT sarcoma were implanted in C57BL/6 mice and WR was inoculated at 10^7 pfu/50 μL (i.t.) at day 1 and day 3 (D1, D3). Serums were harvested on day 1, 3, 5, 7, and 11 (as indicated by "D") and IFNα and IFNβ serum levels were quantified by ProcartaPlex Multiplex Immunoassay following manufacturer's instructions (Thermo Fisher Scientific). Each bar represents the mean of 5 mice/group. **D,** *Ifnar*$^{-/-}$ mice (C57BL/6 background) were implanted with 8×10^5 *Ifnar*$^{-/-}$ MCA205 cells (clone 7) and intratumorally treated as before with WR or buffer on day 0 and day 3. Tumor size (left) and percentages of surviving mice (right) are depicted. Tumor sizes are shown as means ± SEM. Results shown are representative of two independent experiments. *, $P < 0.05$; **, $P < 0.01$; ***, $P < 0.001$ by Kruskal–Wallis test, followed by Dunn post test in **B** (left), by Mann–Whitney test in **C**, or by Kaplan–Meier analysis and log-rank Mantel–Cox test in **B** and **C** (right).

viral replication (Supplementary Fig. S2). In contrast, tumoral TLR3 receptors, which recognize single-strand RNA, did not appear to be needed for the activity of WR (Supplementary Fig. S3).

We studied the role of type I IFN signaling at later stages, that is, once viral replication is supposed to be entailed, through administration of an IFNAR-blocking mAb at days 5 and 10 after WR treatment. Such blockade of the receptor was seen to reduce efficacy of WR and thus to suppress its benefit in term of survival (Fig. 3B). We monitored serum levels of type 1 IFNs and found detectable levels of these viral cytokines, 3–4 days after 2 local inoculations of WR (Fig. 3C), suggesting systemic effects of viral and/or immune-mediated remodeling of the tumor microenvironment post-WR

Published OnlineFirst May 23, 2017; DOI: 10.1158/0008-5472.CAN-16-2165

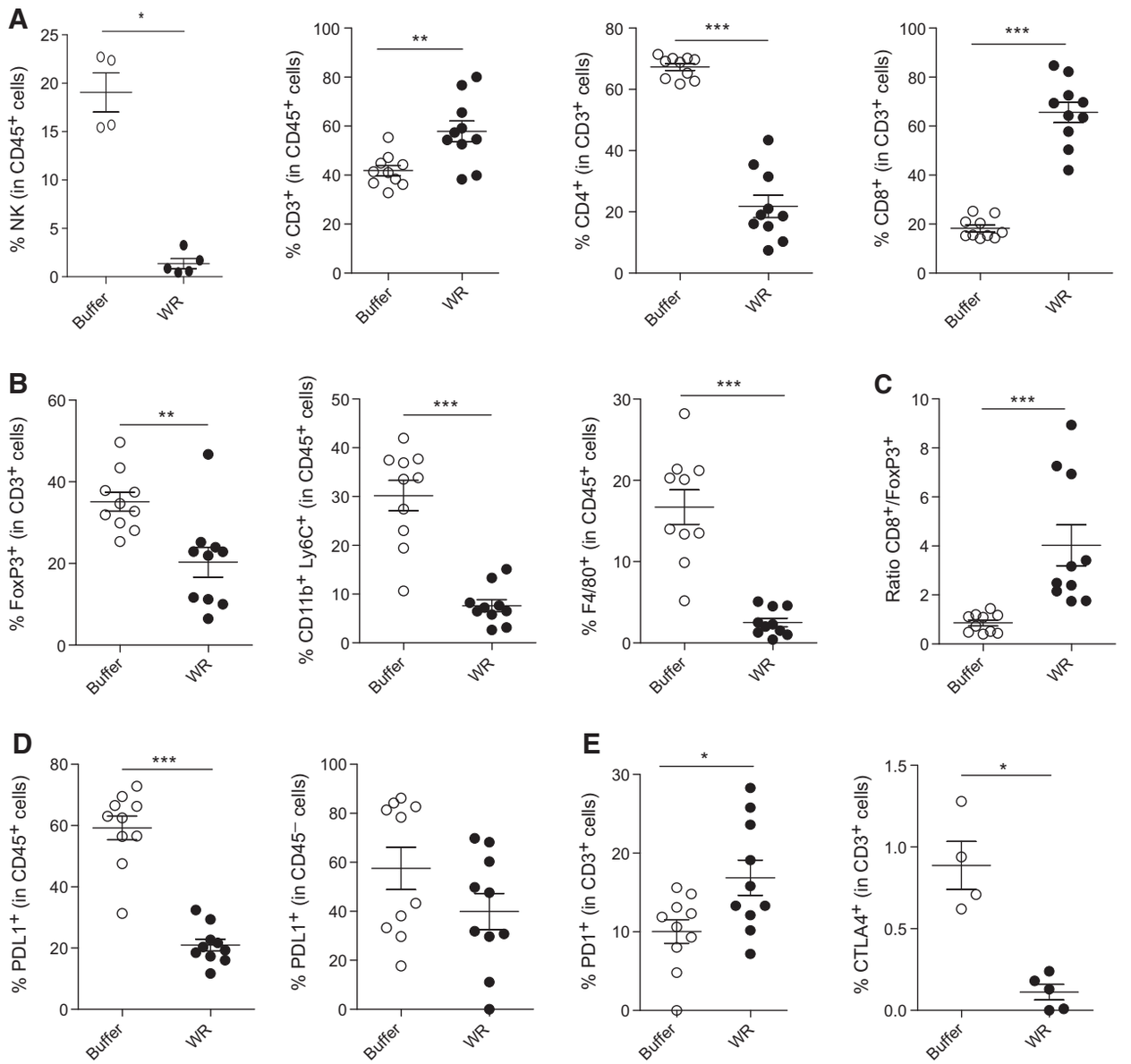

Figure 4.

Characterization of tumor-infiltrating cells following intratumoral WR treatment. C57BL/6 mice were implanted with 8×10^5 MCA205 tumor cells. When tumors reached approximatively 40 mm^2, mice were intratumorally treated with 10^7 pfu WR on day 0 and day 3. Four days after the last injection of WR, tumors were processed for flow cytometry determination of the percentages of NK cells, $CD3^+$ T lymphocytes, and $CD4^+$ and $CD8^+$ (**A**) T cells. The percentage of $FoxP3^+$ regulatory T cells (Tregs), intratumoral myeloid-derived suppressor cells, the percentage of $F4/80^+$ macrophages (**B**), and the ratio of $CD8^+$ T cells to Treg cells (**C**) is also shown. The expression of PD-L1 on leukocytes and on tumor cells (**D**) was determined as well as the expression of the immune checkpoints PD-1 and CTLA-4 (**E**). Results are representative of two independent experiments comprising 5–6 mice/group. *, $P < 0.05$; **, $P < 0.01$; ***, $P < 0.001$ by Mann–Whitney test.

intratumoral inoculation. These results were corroborated using *Ifnar*$^{-/-}$ hosts. The tumor control seen on WR treatment of *Ifnar*$^{-/-}$ MCA205 sarcomas was, however, still present when these tumors were established in *Ifnar*$^{-/-}$ mice, but less prominent than in wild-type animals (Fig. 3D).

Intratumoral injection of WR into established MCA205 tumors in WT mice was seen to significantly alter immune cell populations within the tumor microenvironment (TME), particularly infiltrated lymphocytes and myeloid cells. Hence, 7 days after WR treatment, the percentage of lymphocytes ($CD3^+$, $CD45^+$) was almost twice that of control, mostly due to increased intratumoral $CD8^+$ T cells at the expense of CD4+ T cells and NK cells (Fig. 4A). In contrast, the regulatory components of TME, that is, $CD4^+$ $Foxp3^+$ T cells, $CD11b^+Ly6c^+$, and $F4/80^+$ macrophages, drastically decreased upon WR treatment (Fig. 4B). This translated into a significant increase in the ratio of effectors to regulatory T cells,

Published OnlineFirst May 23, 2017; DOI: 10.1158/0008-5472.CAN-16-2165

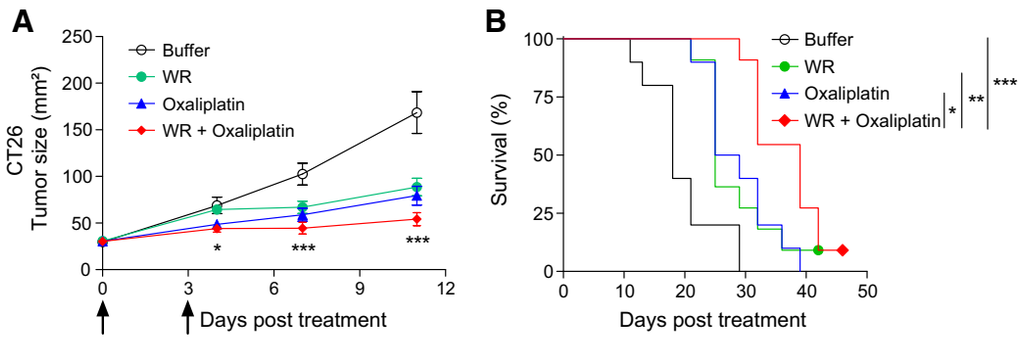

Figure 5.

The antitumor activity of WR is enhanced on combination with oxaliplatin chemotherapy. BALB/c mice were implanted with 8×10^5 CT26 tumor cells. When tumors reached approximatively 40 mm^2, mice were intratumorally treated with 10^7 pfu WR on day 0 and day 3. At day 6, mice were injected with 10 mg/kg/mouse oxaliplatin. Tumor sizes (**A**; shown as means ± SEM) and percentages of surviving mice (**B**) are shown. Results are representative of two independent experiments comprising 5–6 mice/group. *, $P < 0.05$; **, $P < 0.01$; ***, $P < 0.001$ by Kruskal–Wallis test, followed by Dunn post test in **A**, or by Kaplan–Meier analysis and log-rank Mantel–Cox test in **B**.

that is, $CD8^+/Foxp3^+$ (Fig. 4C). WR drastically changed the PD-L1 status in $CD45^+$ infiltrated cells, but not in the $CD45^-$ fraction (Fig. 4D). Of note, WR infection boosted the transcription of type 1 IFN gene products in tumor cells (proficient or deficient for IFNAR), but failed to upregulate PD-L1 expression on tumor cells *in vitro* (not shown). However, WR did not compromise the upregulation of PD-L1–caused type 2 IFN (produced by effector T cells in the TME, not shown). The reduction of PD-L1 expression in the leukocytic fraction might be due to the loss of dendritic cells, expressing the highest levels of PD-L1 (not shown) while the lack of type 1 IFN-induced PD-L1 expression could be explained by a direct quenching of IFN by B18R harbored by WR. Regarding other checkpoint makers, PD1 was increased while CTLA-4 largely decreased in $CD3^+$ lymphoid cells following WR treatment (Fig. 4E).

The therapeutic activity of WR could be further improved by combination with other immunostimulatory agents. Oxaliplatin is known to induce a strong ICD and we could see that combining WR with oxaliplatin resulted in a synergistic improvement of tumor control and survival over monotherapy (Fig. 5). Combination of WR with a PD-1 blocker similarly showed an improved efficacy in terms of increased survival in established MCA205 sarcoma model (Fig. 6A). In line with the previous observation of an increased PD-1 expression in $CD3^+$ TILs (Fig. 4E), we identified that later administration of anti-PD-1 mAbs, after treatment with WR improved its effect (Fig. 6B; Supplementary Fig. S4A). Furthermore, the combination with anti-PD-1 appeared to allow a dose-sparing (Supplementary Fig. S4A). The combination with anti-CTLA-4 also showed an enhanced survival over monotherapy in the same MCA205 sarcoma model. The schedule was important in the combinatorial regimen, requiring blockade of CTLA-4 mAb after WR treatment (Fig. 6C and D). Importantly, the greatest synergistic therapeutic effect in terms of tumor control was achieved when anti-CTLA-4 was administered shortly (1 day) after WR treatment, maybe in relation with the concomittant provision of IL2 [released during CTLA4 blockade (35) and type 1 IFN by the virally infected cells (36)]. The benefit was lost when anti-CTLA-4 was delivered late, 7 days after WR treatment (Supplementary Fig. S4B).

A key aspect to the success of oncolytic virotherapy, either as standalone or as combination therapy, is the ability to induce a systemic anticancer immunity that allows for an abscopal effect on distant tumors/metastases. In this respect, we assessed the abscopal effect of several combination regimens. Considering that the most effective abscopal responses presumably follow a complete response at the initial tumor site, we used MCA205 *Ifnar*$^{-/-}$, that completely regress on WR treatment, as initial tumor in the ipsilateral flank, and challenged the regression of wild-type tumor in the contralateral flank (Fig. 7A). Regimens combining WR with anti-PD-1, anti-CTLA-4, or oxaliplatin each conferred a better control of contralateral tumor growth, compared with WR monotherapy with control antibody (Fig. 7B). Most importantly, each combination regimen displayed higher survival than WR treatment alone (Fig. 7C).

Discussion

We here report that WR, a surrogate model for the preclinical study of TG6002, a first-in class oncolytic poxvirus, is able to induce immunogenic cell death and to beneficially reprogram cell populations within the tumor microenvironment. Moreover, we demonstrate that WR, alone or in combination with oxaliplatin or immune checkpoint blockers, produces abscopal effects on distant untreated tumors, particularly when the treated tumor displays attenuated type I IFN signaling.

The ability for a locally administered therapy to induce an immune-mediated regression of distant neoplasms will strongly determine its clinical success. Accordingly, a complete response at the initial site of local treatment is a prerequisite to secondary abscopal effects. We here confirm that DAMPs, as key immunostimulatory signals representative of ICD, are released upon treatment with WR. The level of ICD was related to WR load and replication, which might explain why injection of WR into *Ifnar*$^{-/-}$ tumors (allowing for increased OV susceptibility and replication; ref. 37) led to complete regression of the injected tumor and conveyed effective abscopal effects on distant IFNAR-competent tumors. However, in apparent contrast with this, blockade of IFNAR after WR treatment resulted in lower tumor control. This suggests the requirement of a later, intact type I IFN response for the propagation of antitumor immune responses after ICD, as already reported with other oncolytic viruses (38, 39). Presumably, this drove chemokine secretion and subsequent

Published OnlineFirst May 23, 2017; DOI: 10.1158/0008-5472.CAN-16-2165

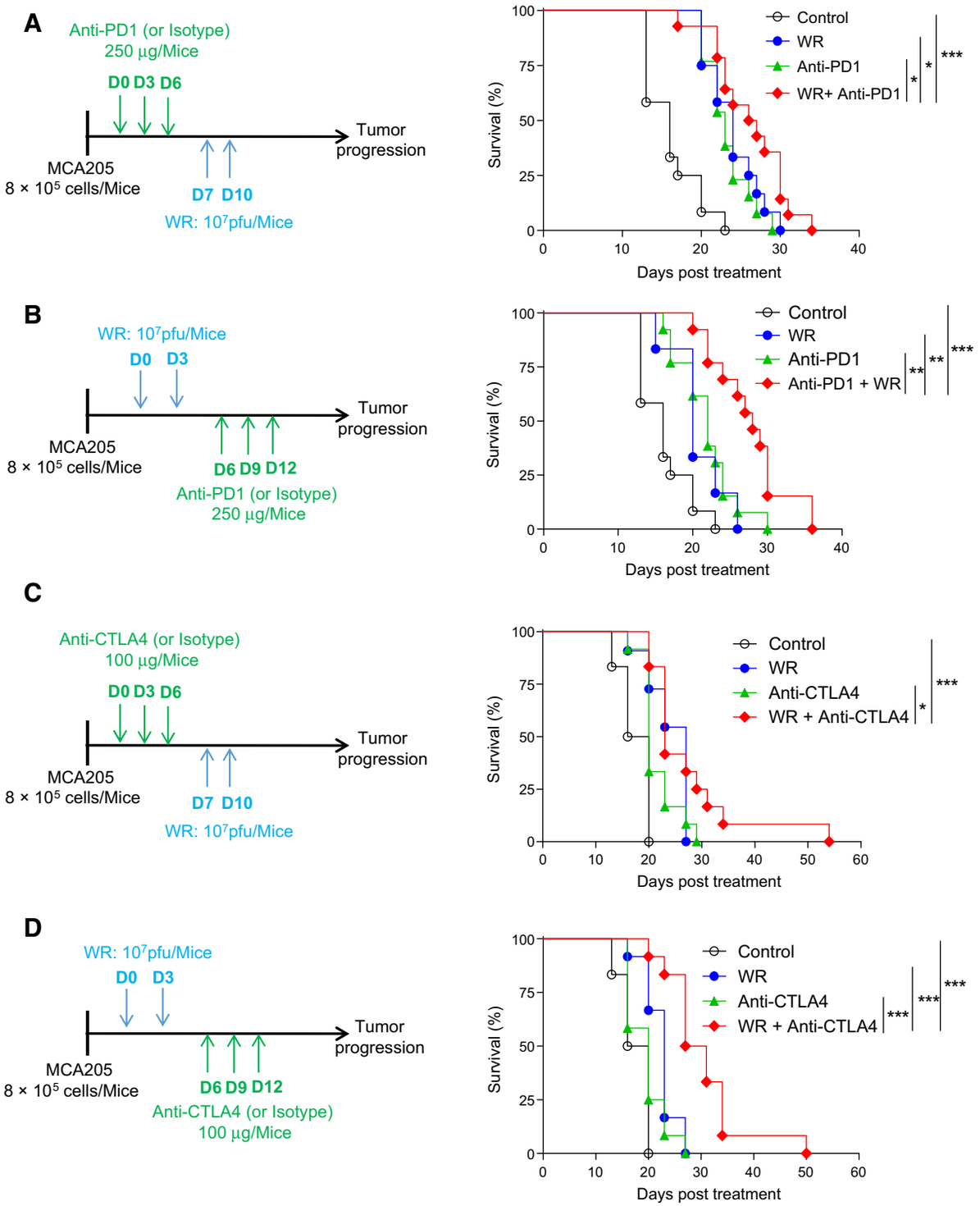

Figure 6.

Combination of WR with immune checkpoint blockers increases therapeutic activity. **A,** C57BL/6 mice with established MCA205 tumors were treated (i.p.) with 250 μg/mouse anti-PD-1 mAb on day 0, 3, and 6. At day 7 and 10, mice were intratumorally administered 10^7 pfu WR, and their survival was monitored as shown (right). **B,** Similar to **A**, but with mice treated with WR before anti-PD-1 mAb treatment. **C,** Similar experimental design to **A**, but mice treated with 100 μg/mouse (i.p.) of anti-CTLA4 mAb on day 0, 3, and 6 before WR treatment on day 7 and 10. **D,** Similar to **B**, but mice treated with WR before anti-CTLA4 mAb treatment. Results are representative of two independent experiments comprising 5–6 mice/group. *, $P < 0.05$; **, $P < 0.01$; ***, $P < 0.001$ by Kaplan–Meier analysis and log-rank Mantel–Cox test in **B**.

Published OnlineFirst May 23, 2017; DOI: 10.1158/0008-5472.CAN-16-2165

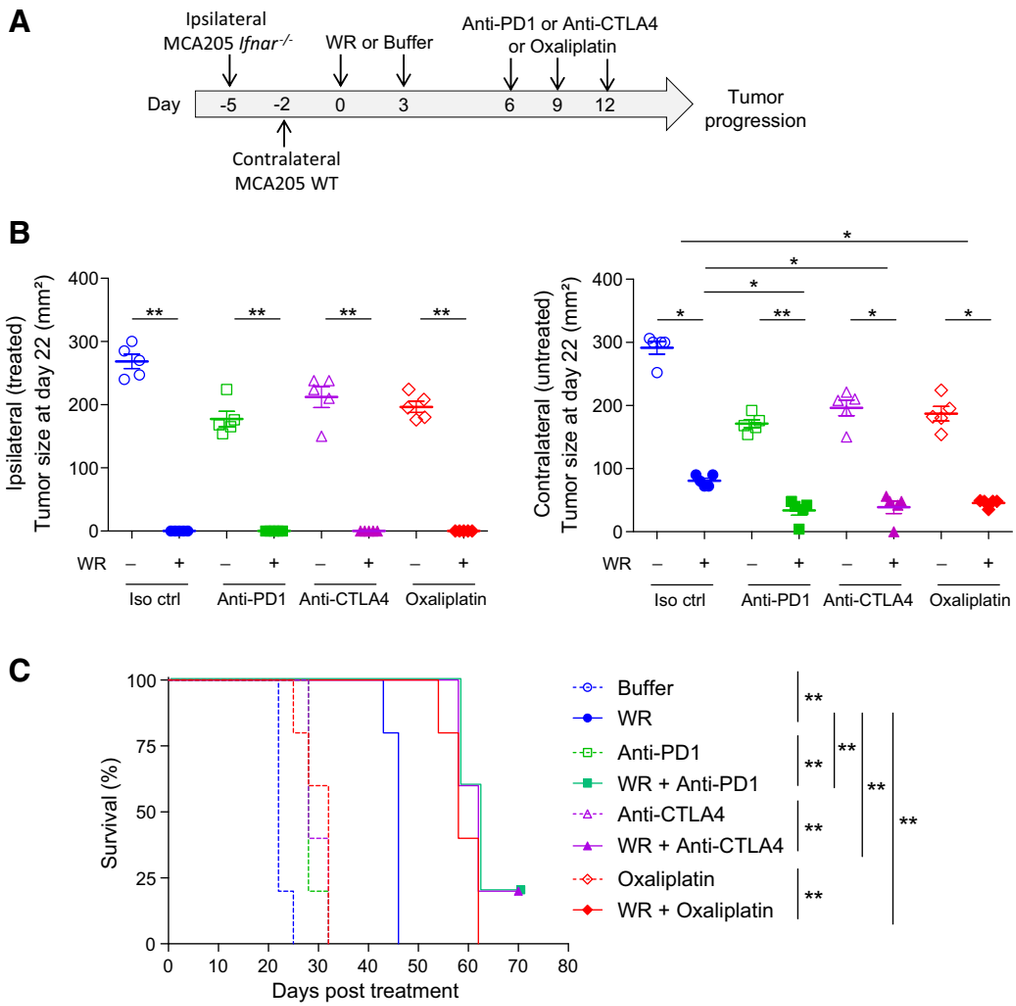

Figure 7.

Abscopal response in an IFNAR-defective environment after local therapy with WR and immune checkpoint blockers. **A,** C57BL/6 mice were implanted with 8×10^5 MCA205 *Ifnar*$^{-/-}$ cells on one flank and 3 days after with 8×10^5 MCA205 WT cells on the opposite flank. When MCA205 *Ifnar*$^{-/-}$ tumors reached approximately 20 mm^2, mice were intratumorally treated with 10^7 pfu WR on day 0 and day 3. Mice were administrated with 250 μg/mouse anti-PD-1 mAb (at day 6, 9 and 12), with 100 μg/mouse anti-CTLA4 mAb (at day 6, 9, and 12) or with 10 mg/kg/mouse oxaliplatin (at day 6). **B,** Tumor sizes in the ipsilateral (treated, left) or contralateral (untreated, right) are shown as means ± SEM. **C,** Kaplan–Meier curves of mouse survival following the combination regimes are depicted. The experiments were performed twice with similar results. *, $P < 0.05$; **, $P < 0.01$; ***, $P < 0.001$ by Kruskal–Wallis test, followed by Dunn post test in **B**, or by Kaplan–Meier analysis and log-rank Mantel–Cox test in **C**.

T-cell recruiting, as well as activation of APCs and presentation of tumor antigen to T cells (31, 40, 41).

Combination of OVs with either checkpoint blockers or immunogenic chemotherapy is an appealing approach to boost the immune response initiated at the level of the treated tumor. A similar combinatory approach supports this view; administration of ICD-inducing chemotherapies ahead of ICB therapy has been observed to transform tumors into enhanced immunologic areas with significant T-cell infiltration (i.e., restoring a high T effector cell/Treg cell ratio), resulting in an improved ICB-mediated inhibition of tumor progression (42).

Our study provides a rationale for combination of oncolytic therapy and ICBs for several reasons: (i) WR upregulates the expression of PD-1 on T cells; (ii) combination of anti-PD-1 and WR displayed therapeutic synergy and abscopal effects; (iii) this synergy allowed for a 10-fold reduction of WR, an advantageous dose-sparing effect; (iv) both the therapeutic action and abscopal effects of WR could similarly be increased through blockade of CTLA-4.

Moreover, we show that the schedule is important; CTLA-4 blockade worked best shortly after WR treatment, whereas PD-1 blockade worked better when delivered later, that is, 7 days after WR treatment. These findings may reflect the time-dependent regulation of these markers as we identified that expression of CTLA-4 is significantly downregulated in T cells after 7 days, while PD-1 showed increased expression for longer period. The requirement for early blockade of CTLA-4 may be explained by the fact that anti-CTLA-4 mAbs deplete Treg cells from the TME (43), and

Published OnlineFirst May 23, 2017; DOI: 10.1158/0008-5472.CAN-16-2165

increase the recruitment of antitumor and antiviral CTLs within the next days.

The depletion of Treg cells may indeed be key to the success of OV therapy, removing a regulatory hurdle on the WR-initiated $CD8^+$ T-cell response (this also potentially explaining why $CD4^+$ T-cell depletion in our model was not deleterious to the therapeutic action of WR). Local delivery of anti-CTLA-4 may be desirable considering the systemic toxicity of ipilimumab (44). Our results also support our vectorization strategy that locally delivers anti-PD-1 encoded by an OV directly within the TME (Fend and colleagues, in press). Two ongoing clinical trials in unresectable melanoma patients, a phase I/II study of T-VEC in combination with systemic ipilimumab (NCT01740297; ref. 45) and a phase III study exploring the combination of T-VEC with systemic pembrolizumab (NCT02263508; refs. 45, 46), will substantiate our findings.

Finally, our results suggest that oncolytic virotherapy can be targeted to tumors, which are defective in the IFNAR pathway. IHC offers a rather easy way to assess type I IFN signaling component; for example, phospho-STAT-1 and MxA (31, 40). Screening of type I IFN signaling activity in tumors may therefore become a useful approach to help decision of OV treatment, direct the protocol, and predict therapeutic response.

Disclosure of Potential Conflicts of Interest

X. Préville is the head of the Oncoimmunology Department and has ownership interest (including patents) in Transgene. A. Marabelle has received speakers bureau honoraria from Amgen and is a consultant/advisory board member for Amgen and Transgene. L. Zitvogel is a member of board of administration at Transgene and is a consultant/advisory board member for Lytix Pharma. No potential conflicts of interest were disclosed by the other authors.

Authors' Contributions

Conception and design:L. Fend, T. Yamazaki, G. Kroemer, L. Zitvogel
Development of methodology:L. Fend, T. Yamazaki, O. Kepp, L. Zitvogel
Acquisition of data (provided animals, acquired and managed patients, provided facilities, etc.):L. Fend, T. Yamazaki, X. Préville, O. Kepp
Analysis and interpretation of data (e.g., statistical analysis, biostatistics, computational analysis):L. Fend, T. Yamazaki, E. Quéméneur, J. Adam, A. Marabelle, L. Zitvogel
Writing, review, and/or revision of the manuscript:L. Fend, T. Yamazaki, X. Préville, E. Quéméneur, J.M. Pitt, G. Kroemer, L. Zitvogel
Administrative, technical, or material support (i.e., reporting or organizing data, constructing databases):T. Yamazaki, C. Remy, C. Fahrner, M. Gantzer, V. Nourtier, X. Préville, E. Quéméneur
Study supervision:L. Fend, E. Quéméneur, A. Marabelle, J.M. Pitt, L. Zitvogel

Acknowledgments

We thank the unknown reviewers for their help to ameliorate this article. We also appreciate the help from animal facility in Institut Gustave Roussy and Berangere Marie-Bastien for the statistical analysis of the data.

Grant Support

Transgene supported experimental expenses at Gustave Roussy Cancer Center. J.M. Pitt is supported by ARC. G. Kroemer and L. Zitvogel were supported by the Ligue Nationale contre le Cancer (Equipes labellisées), Agence Nationale pour la Recherche (ANR AUTOPH, ANR Emergence), European Commission (ArtForce), European Research Council Advanced Investigator Grant (to G. Kroemer), Fondation pour la Recherche Médicale (FRM), Institut National du Cancer (INCa), Fondation de France, Cancéropôle Ile-de-France, Fondation Bettencourt-Schueller, Swiss Bridge Foundation, the LabEx Immuno-Oncology, the SIRIC Stratified Oncology Cell DNA Repair and Tumor Immune Elimination (SOCRATE); the SIRIC Cancer Research and Personalized Medicine (CARPEM), and the Paris Alliance of Cancer Research Institutes (PACRI). L. Zitvogel and G. Kroemer are sponsored by Association pour la Recherche contre le Cancer (PGA120140200851) and ISREC Foundation.

The costs of publication of this article were defrayed in part by the payment of page charges. This article must therefore be hereby marked *advertisement* in accordance with 18 U.S.C. Section 1734 solely to indicate this fact.

Received August 5, 2016; revised February 8, 2017; accepted May 17, 2017; published OnlineFirst May 23, 2017.

References

1. Pol J, Kroemer G, Galluzzi L. First oncolytic virus approved for melanoma immunotherapy. Oncoimmunology 2016;5:e1115641.
2. Lichty BD, Breitbach CJ, Stojdl DF, Bell JC. Going viral with cancer immunotherapy. Nat Rev Cancer 2014;14:559–67.
3. Pikor LA, Bell JC, Diallo J-S. Oncolytic viruses: exploiting cancer's deal with the devil. Trends Cancer 2015;1:266–77.
4. Power AT, Bell JC. Taming the Trojan horse: optimizing dynamic carrier cell/oncolytic virus systems for cancer biotherapy. Gene Ther 2008;15: 772–9.
5. Marcato P, Shmulevitz M, Pan D, Stoltz D, Lee PW. Ras transformation mediates reovirus oncolysis by enhancing virus uncoating, particle infectivity, and apoptosis-dependent release. Mol Ther 2007;15: 1522–30.
6. Garant KA, Shmulevitz M, Pan L, Daigle RM, Ahn DG, Gujar SA, et al. Oncolytic reovirus induces intracellular redistribution of Ras to promote apoptosis and progeny virus release. Oncogene 2016;35:771–82.
7. Shmulevitz M, Lee PW. Exploring host factors that impact reovirus replication, dissemination, and reovirus-induced cell death in cancer versus normal cells in culture. Methods Mol Biol 2012;797:163–76.
8. Roulstone V, Pedersen M, Kyula J, Mansfield D, Khan AA, McEntee G, et al. BRAF- and MEK-targeted small molecule inhibitors exert enhanced anti-melanoma effects in combination with oncolytic reovirus through ER stress. Mol Ther 2015;23:931–42.
9. Kanerva A, Nokisalmi P, Diaconu I, Koski A, Cerullo V, Liikanen I, et al. Antiviral and antitumor T-cell immunity in patients treated with GM-CSF-coding oncolytic adenovirus. Clin Cancer Res 2013;19:2734–44.
10. Kim MK, Breitbach CJ, Moon A, Heo J, Lee YK, Cho M, et al. Oncolytic and immunotherapeutic vaccinia induces antibody-mediated complement-dependent cancer cell lysis in humans. Sci Transl Med 2013; 5:185ra63.
11. Kleijn A, Kloezeman J, Treffers-Westerlaken E, Fulci G, Leenstra S, Dirven C, et al. The in vivo therapeutic efficacy of the oncolytic adenovirus Delta24-RGD is mediated by tumor-specific immunity. PLoS One 2014;9:e97495.
12. Liikanen I, Ahtiainen L, Hirvinen ML, Bramante S, Cerullo V, Nokisalmi P, et al. Oncolytic adenovirus with temozolomide induces autophagy and antitumor immune responses in cancer patients. Mol Ther 2013; 21:1212–23.
13. Moehler MH, Zeidler M, Wilsberg V, Cornelis JJ, Woelfel T, Rommelaere J, et al. Parvovirus H-1-induced tumor cell death enhances human immune response in vitro via increased phagocytosis, maturation, and cross-presentation by dendritic cells. Hum Gene Ther 2005;16:996–1005.
14. Kroemer G, Galluzzi L, Kepp O, Zitvogel L. Immunogenic cell death in cancer therapy. Annu Rev Immunol 2013;31:51–72.
15. Fend L, Remy-Ziller C, Foloppe J, Kempf J, Cochin S, Barraud L, et al. Oncolytic virotherapy with an armed vaccinia virus in an orthotopic model of renal carcinoma is associated with modification of the tumor microenvironment. Oncoimmunology 2016;5:e1080414.
16. Galluzzi L, Senovilla L, Zitvogel L, Kroemer G. The secret ally: immunostimulation by anticancer drugs. Nat Rev Drug Discov 2012;11:215–33.
17. Minn AJ. Interferons and the immunogenic effects of cancer therapy. Trends Immunol 2015;36:725–37.
18. Hiniker SM, Chen DS, Knox SJ. Abscopal effect in a patient with melanoma. N Engl J Med 2012;366:2035.
19. Postow MA, Callahan MK, Barker CA, Yamada Y, Yuan J, Kitano S, et al. Immunologic correlates of the abscopal effect in a patient with melanoma. N Engl J Med 2012;366:925–31.

20. Stamell EF, Wolchok JD, Gnjatic S, Lee NY, Brownell I. The abscopal effect associated with a systemic anti-melanoma immune response. Int J Radiat Oncol Biol Phys 2013;85:293–5.
21. Marabelle A, Kohrt H, Caux C, Levy R. Intratumoral immunization: a new paradigm for cancer therapy. Clin Cancer Res 2014;20:1747–56.
22. Brody JD, Ai WZ, Czerwinski DK, Torchia JA, Levy M, Advani RH, et al. In situ vaccination with a TLR9 agonist induces systemic lymphoma regression: a phase I/II study. J Clin Oncol 2010;28:4324–32.
23. Heo J, Reid T, Ruo L, Breitbach CJ, Rose S, Bloomston M, et al. Randomized dose-finding clinical trial of oncolytic immunotherapeutic vaccinia JX-594 in liver cancer. Nat Med 2013;19:329–36.
24. Park BH, Hwang T, Liu TC, Sze DY, Kim JS, Kwon HC, et al. Use of a targeted oncolytic poxvirus, JX-594, in patients with refractory primary or metastatic liver cancer: a phase I trial. Lancet Oncol 2008;9:533–42.
25. Kaufman HL, Amatruda T, Reid T, Gonzalez R, Glaspy J, Whitman E, et al. Systemic versus local responses in melanoma patients treated with talimogene laherparepvec from a multi-institutional phase II study. J Immunother Cancer 2016;4:12.
26. Andtbacka RH, Kaufman HL, Collichio F, Amatruda T, Senzer N, Chesney J, et al. Talimogene laherparepvec improves durable response rate in patients with advanced melanoma. J Clin Oncol 2015;33:2780–8.
27. Marabelle A, Kohrt H, Sagiv-Barfi I, Ajami B, Axtell RC, Zhou G, et al. Depleting tumor-specific Tregs at a single site eradicates disseminated tumors. J Clin Invest 2013;123:2447–63.
28. Zamarin D, Holmgaard RB, Subudhi SK, Park JS, Mansour M, Palese P, et al. Localized oncolytic virotherapy overcomes systemic tumor resistance to immune checkpoint blockade immunotherapy. Sci Transl Med 2014;6:226ra32.
29. Foloppe J, Kintz J, Futin N, Findeli A, Cordier P, Schlesinger Y, et al. Targeted delivery of a suicide gene to human colorectal tumors by a conditionally replicating vaccinia virus. Gene Ther 2008;15:1361–71.
30. Shu SY, Rosenberg SA. Adoptive immunotherapy of newly induced murine sarcomas. Cancer Res 1985;45:1657–62.
31. Sistigu A, Yamazaki T, Vacchelli E, Chaba K, Enot DP, Adam J, et al. Cancer cell-autonomous contribution of type I interferon signaling to the efficacy of chemotherapy. Nat Med 2014;20:1301–9.
32. Apetoh L, Ghiringhelli F, Tesniere A, Obeid M, Ortiz C, Criollo A, et al. Toll-like receptor 4-dependent contribution of the immune system to anticancer chemotherapy and radiotherapy. Nat Med 2007;13:1050–9.
33. Michaud M, Martins I, Sukkurwala AQ, Adjemian S, Ma Y, Pellegatti P, et al. Autophagy-dependent anticancer immune responses induced by chemotherapeutic agents in mice. Science 2011;334:1573–7.
34. Ghiringhelli F, Apetoh L, Tesniere A, Aymeric L, Ma Y, Ortiz C, et al. Activation of the NLRP3 inflammasome in dendritic cells induces IL-1beta-dependent adaptive immunity against tumors. Nat Med 2009;15:1170–8.
35. Hannani D, Vetizou M, Enot D, Rusakiewicz S, Chaput N, Klatzmann D, et al. Anticancer immunotherapy by CTLA-4 blockade: obligatory contribution of IL-2 receptors and negative prognostic impact of soluble CD25. Cell Res 2015;25:208–24.
36. Kottke T, Diaz RM, Kaluza K, Pulido J, Galivo F, Wongthida P, et al. Use of biological therapy to enhance both virotherapy and adoptive T-cell therapy for cancer. Mol Ther 2008;16:1910–8.
37. Vähä-Koskela M, Hinkkanen A. Tumor restrictions to oncolytic virus. Biomedicines 2014;2:163.
38. Wongthida P, Diaz RM, Galivo F, Kottke T, Thompson J, Pulido J, et al. Type III IFN interleukin-28 mediates the antitumor efficacy of oncolytic virus VSV in immune-competent mouse models of cancer. Cancer Res 2010;70:4539–49.
39. Wongthida P, Diaz RM, Galivo F, Kottke T, Thompson J, Melcher A, et al. VSV oncolytic virotherapy in the B16 model depends upon intact MyD88 signaling. Mol Ther 2011;19:150–8.
40. Zitvogel L, Galluzzi L, Kepp O, Smyth MJ, Kroemer G. Type I interferons in anticancer immunity. Nat Rev Immunol 2015;15:405–14.
41. Diamond MS, Kinder M, Matsushita H, Mashayekhi M, Dunn GP, Archambault JM, et al. Type I interferon is selectively required by dendritic cells for immune rejection of tumors. J Exp Med 2011;208:1989–2003.
42. Pfirschke C, Engblom C, Rickelt S, Cortez-Retamozo V, Garris C, Pucci F, et al. Immunogenic chemotherapy sensitizes tumors to checkpoint blockade therapy. Immunity 2016;44:343–54.
43. Simpson TR, Li F, Montalvo-Ortiz W, Sepulveda MA, Bergerhoff K, Arce F, et al. Fc-dependent depletion of tumor-infiltrating regulatory T cells co-defines the efficacy of anti-CTLA-4 therapy against melanoma. J Exp Med 2013;210:1695–710.
44. Weber JS, Kahler KC, Hauschild A. Management of immune-related adverse events and kinetics of response with ipilimumab. J Clin Oncol 2012;30:2691–7.
45. Pol J, Buque A, Aranda F, Bloy N, Cremer I, Eggermont A, et al. Trial Watch-Oncolytic viruses and cancer therapy. Oncoimmunology 2016;5:e1117740.
46. Zou W, Wolchok JD, Chen L. PD-L1 (B7-H1) and PD-1 pathway blockade for cancer therapy: mechanisms, response biomarkers, and combinations. Sci Transl Med 2016;8:328rv4.

Published OnlineFirst May 23, 2017; DOI: 10.1158/0008-5472.CAN-16-2165

Cancer Research
The Journal of Cancer Research (1916–1930) | The American Journal of Cancer (1931–1940)

AACR American Association for Cancer Research

Immune Checkpoint Blockade, Immunogenic Chemotherapy or IFN-α Blockade Boost the Local and Abscopal Effects of Oncolytic Virotherapy

Laetitia Fend, Takahiro Yamazaki, Christelle Remy, et al.

Cancer Res 2017;77:4146-4157. Published OnlineFirst May 23, 2017.